



Check for updates

Theoretical Physics. Quantum Mechanics

UDC 517.938

EDN KZISPS

<https://www.doi.org/10.33910/2687-153X-2022-3-4-186-201>

Atmospheric implementation of superdense coding quantum algorithm

B. A. Timchenko¹, M. P. Faleeva¹, P. A. Gilev¹, I. V. Blinova¹, I. Yu. Popov^{✉1}

¹ ITMO University, 49 Kronverksky Ave., Saint Petersburg 197101, Russia

Authors

Bogdan A. Timchenko, e-mail: bogdantimchenko@yandex.ru

Maria P. Faleeva, e-mail: faleeva.masha@gmail.com

Pavel A. Gilev, e-mail: grandarchtemplar@gmail.com

Irina V. Blinova, e-mail: irin-a@yandex.ru

Igor Yu. Popov, ORCID: [0000-0002-5251-5327](https://orcid.org/0000-0002-5251-5327), e-mail: popov1955@gmail.com

For citation: Timchenko, B. A., Faleeva, M. P., Gilev, P. A., Blinova, I. V., Popov, I. Yu. (2022) Atmospheric implementation of superdense coding quantum algorithm. *Physics of Complex Systems*, 3 (4), 186–201. <https://www.doi.org/10.33910/2687-153X-2022-3-4-186-201> EDN KZISPS

Received 12 September 2022; reviewed 2 October 2022; accepted 2 October 2022.

Funding: The work was partially supported by grant No. 19-31-90154 of the Russian Foundation for Basic Research.

Copyright: © B. A. Timchenko, M. P. Faleeva, P. A. Gilev, I. V. Blinova, I. Yu. Popov (2022). Published by Herzen State Pedagogical University of Russia. Open access under [CC BY-NC License 4.0](https://creativecommons.org/licenses/by-nc/4.0/).

Abstract. We consider the properties of a quantum communication channel in open space using the superdense coding algorithm as an example. We studied the theoretical model of the installation that implements this algorithm, and identified the main factors affecting the quality of the model. Among them is the atmospheric transmittance, the efficiency of detectors, and the average value of the number of noise counts caused by background radiation and dark counts. We made a complete calculation of the installation model and obtained explicit results. These results were analyzed using realistic parameters of detectors and the atmosphere. It was found that the atmospheric turbulence instability, detectors efficiency and the average value of noise counts have the greatest influence on the results.

Keywords: quantum channel, dense coding, entanglement, atmosphere, model

Introduction

At the moment, processors with 10 nm manufacturing technology are already widespread, which corresponds to literally several tens of silicon atoms. These sizes are so small that fundamental difficulties are already appearing that introduce quantum effects. A possible solution to this problem is the transition to another computing paradigm. Recently, the quantum theory of information, which provides a similar paradigm, has been central to many studies. However, there still is a number of unresolved issues related, in particular, to network interaction between processors of quantum information. Networking is one of the most important components of computing systems that allows for scalable growth. This role is preserved in quantum networks. Of course, the functional elements that provide communication between nodes change. From examples of use, we can distinguish distributed quantum computing and the quantum distribution of keys used in cryptography. The possibility of implementing the latter using quantum communication channels formed by polarized photons in open space was recently shown experimentally (Elser et al. 2009; Fedrizzi et al. 2009; Ursin et al. 2007). This raises the question of preserving the nonclassical properties of light as it passes through fluctuating media. Generated by Kolmogorov's theory of turbulence, the theory of classical light transmission through the atmosphere

has been studied for a long time (Ishimaru 1978; Tatarskii 1971). Compared to it, the theory of transmission of quantum light in random media is less developed. A theoretical model of light passing through a turbulent atmosphere and processed by homodyne detection has recently been proposed (Semenov et al. 2008; 2009). It describes random media and fluctuating loss channels that introduce additional noise into the quantum states of light in comparison with standard channels. Such noise was discovered in (Dong et al. 2008; Heersink et al. 2006). In this paper, we study the transfer of entanglement by photons through a turbulent atmosphere using fluctuating loss channels. The relevance of this issue lies in the fact that quantum networks are attracting an increasing interest, and theoretical noise estimates can give a more realistic forecast of experimental data (Adam et al. 2022, Fedrizzi et al. 2009; Gilev, Popov 2019; Herbst et al. 2015). The object of the study was a scheme that implements a superdense coding algorithm. The choice is due to the fact that this scheme uses quantum communication channels to achieve the results that have no analogue using classical channels. In addition, the results of the scheme work can be presented in a simpler form. These results are the subject of research, namely, the probability of postselective detection of various pairs of bits depending on the transmitted pair. The aim of the work is to investigate the dependence of the probabilities defined above on the parameters of a turbulent atmosphere.

The work is structured as follows. Section 2 provides an overview of the superdense coding algorithm, its physical implementation, and analysis of factors that impact the final result. In section 3, we calculate the matrix of the density of states of the system at all stages, detect the resulting state on a linear Bell state meter and obtain the probabilities indicated in the purpose of this study.

Theoretical background

Device description

Superdense coding is an algorithm that allows you to transfer two bits of classical information by sending only one qubit, under the assumption that Alice and Bob prepared and shared an entangled state. The transmission of two bits is possible due to the quantum intricacies of the qubits. It was developed by (Bennett, Wiesner 1992) and experimentally implemented in 1996 (Mattle et al. 1996).

The algorithm can be described by the circuit shown in Figure 1. Logically, it consists of three parts. The sender (Alice) wants to send two classical bits of information (00, 01, 10, or 11) to the recipient (Bob) using qubits (instead of classical bits). To do this, she prepares a pair of entangled qubits in the state $|\psi^+\rangle = \frac{1}{\sqrt{2}}(|10\rangle + |01\rangle)$, which is a Bell state using the Hadamard element and CNOT.

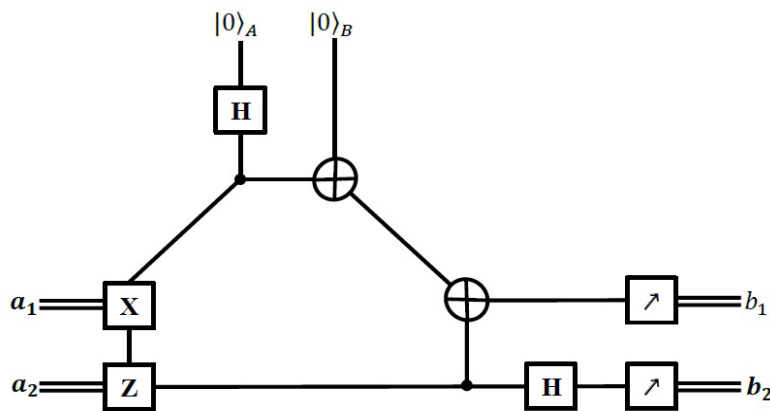


Fig. 1. Quantum circuit for the implementation of superdense coding algorithm

On the left side of the circuit, the first qubit is encoded by Alice by applying the elements X and/or Z . Depending on the transmitted pair of bits, the system of two qubits goes into one of the states:

$$\begin{aligned}
 00: |\psi^+\rangle &\rightarrow |\psi^+\rangle = \frac{1}{\sqrt{2}}(|01\rangle + |10\rangle), \\
 01: |\psi^+\rangle &\rightarrow |\phi^+\rangle = \frac{1}{\sqrt{2}}(|00\rangle + |11\rangle), \\
 10: |\psi^+\rangle &\rightarrow |\psi^-\rangle = \frac{1}{\sqrt{2}}(|01\rangle - |10\rangle), \\
 11: |\psi^+\rangle &\rightarrow |\phi^-\rangle = \frac{1}{\sqrt{2}}(|00\rangle - |11\rangle).
 \end{aligned}$$

These four states are called Bell states, and they form an orthonormal basis, which means that they can be uniquely distinguished by a suitable measurement. After sending the qubits to Bob (by different paths), this measurement is performed on the right side of the circuit using the Hadamard element, CNOT and measuring instruments. All the mentioned quantum elements are described in (Nielsen, Chuang 2010).

The circuit described above works correctly under the condition that there is no noise affecting the state of the system. However, in experimental implementation (Dong et al. 2008; Heersink et al. 2006), noise is inevitable, and errors appear in the operation of the algorithm. This must be considered when using it.

Model background

General remarks

When assessing the effect of noise on the quality of the algorithm, it is necessary to design a model of the installation that executes this algorithm, and note the places where the noise appears and its nature. When modeling quantum circuits, first, it is necessary to solve the question of the carrier of quantum information. In this work, the polarization of a photon is used for qubit coding (Mandel, Wolf 1995), since photons propagate relatively freely in the atmosphere. Note that for atmospheric quantum channels, modes of Gaussian beam can be used for qubit coding (Faleeva, Popov 2020a; 2020b; 2022). As it is known, when coding by polarization states (Semenov, Vogel 2010) a qubit is noted by $\alpha|H\rangle + \beta|V\rangle$ where $|H\rangle$ state means that a photon is in the horizontal mode, $|V\rangle$ state means that a photon is in the vertical mode. This notation is identical to the notation

$$|\psi^+\rangle = \frac{1}{\sqrt{2}}(|1\rangle_{H_A} |0\rangle_{V_A} |0\rangle_{H_B} |1\rangle_{V_B} + |0\rangle_{H_A} |1\rangle_{V_A} |1\rangle_{H_B} |0\rangle_{V_B}),$$

which will be written in simpler form:

$$|\psi^+\rangle = \frac{1}{\sqrt{2}}(|1001\rangle + |0110\rangle). \tag{1}$$

Analogously, the other Bell states for the polarization of photons are as follows:

$$|\phi^+\rangle = \frac{1}{\sqrt{2}}(|1010\rangle + |0101\rangle),$$

$$|\psi^-\rangle = \frac{1}{\sqrt{2}}(|1001\rangle - |0110\rangle),$$

$$|\phi^-\rangle = \frac{1}{\sqrt{2}}(|1010\rangle - |0101\rangle),$$

where the states are presented in the Fock basis and correspond to modes H_A, V_A, H_B and V_B . We take (1) as the initial state.

Alice's part

To model coding at the Alice's part, one should present physical implementation of elements X and Z . Element X performs the operation $\{|0\rangle \rightarrow |1\rangle, |1\rangle \rightarrow |0\rangle\}$. In terms of the annihilation operators it looks as follows $\{\hat{a}_H^{out} = \hat{a}_V^{in}, \hat{a}_V^{out} = \hat{a}_H^{in}\}$. A half-wavelength plate (HWP) can be a model of element X . The Jones matrix for it has the form (Peters et al. 2003):

$$O_{HWP}(\theta) = \begin{pmatrix} -\cos 2\theta & -\sin 2\theta \\ -\sin 2\theta & \cos 2\theta \end{pmatrix},$$

where θ is the angle between the optical axis and the horizontal mode. One has for $\theta = -\frac{\pi}{4}$:

$$O_{HWP}\left(-\frac{\pi}{4}\right) = \begin{pmatrix} 0 & 1 \\ 1 & 0 \end{pmatrix},$$

which corresponds to proper transformation: $\{\hat{a}_H^{out} = \hat{a}_H^{in}, \hat{a}_V^{out} = -\hat{a}_V^{in}\}$.

Element Z performs the transformation $\{|0\rangle \rightarrow |0\rangle, |1\rangle \rightarrow -|1\rangle\} \Leftrightarrow \{\hat{a}_H^{out} = \hat{a}_H^{in}, \hat{a}_V^{out} = -\hat{a}_V^{in}\}$. One can take two 1/4-wavelength plates (QWP) for Z . The corresponding Jones matrix is as follows (Peters et al. 2003):

$$O_{QWP}(\theta) = \begin{pmatrix} 1 - (1+i)\cos^2\theta & -(1+i)\sin\theta\cos\theta \\ -(1+i)\sin\theta\cos\theta & 1 - (1+i)\sin^2\theta \end{pmatrix}.$$

For $\theta = -\frac{\pi}{2}$, one gets:

$$O_{QWP}\left(-\frac{\pi}{2}\right) = \begin{pmatrix} 1 & 0 \\ 0 & -i \end{pmatrix}.$$

For two plates, one has the square of QWP Jones matrix corresponding to proper transformation.

As a result, in a relation with the transmitted bits, the transformations of the annihilation operators at the Alice's side are as follows:

$$\begin{aligned} 00: & \{\hat{a}_H^{out} = \hat{a}_H^{in}, \hat{a}_V^{out} = \hat{a}_V^{in}\}, \\ 01: & \{\hat{a}_H^{out} = \hat{a}_V^{in}, \hat{a}_V^{out} = \hat{a}_H^{in}\}, \\ 10: & \{\hat{a}_H^{out} = \hat{a}_H^{in}, \hat{a}_V^{out} = -\hat{a}_V^{in}\}, \\ 11: & \{\hat{a}_H^{out} = -\hat{a}_V^{in}, \hat{a}_V^{out} = \hat{a}_H^{in}\}. \end{aligned} \tag{2}$$

Bob's part

An implementation of the Bell side is the Bell meter shown in Figure 2.

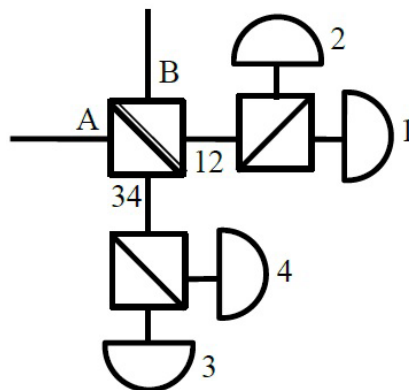


Fig. 2. Copenhagen circuit for Bell measurement

It is important to consider that this model is not perfect, which will be shown below. An alternative is the Kerr medium for photon interaction (Nielsen, Chuang 2010) or the use of photon hyper-entanglement, as was done in 2001 (Williams et al. 2018), to unambiguously distinguish Bell states. The main elements of this measuring device are as follows: a symmetric beam splitter, two polarizing beam splitters and four detectors operating in the photon counting mode. The role of the symmetric beam splitter in this measurement is the interference of the photons of the incoming modes A and B . In fact, this means that the sum and the difference of the two fields are formed at the outputs. Relations between the operators at the input and output are as follows (Schleich 2001):

$$\hat{a}_1 = \frac{1}{\sqrt{2}}(\hat{a}_{HA} + \hat{a}_{HB}), \quad \hat{a}_2 = \frac{1}{\sqrt{2}}(\hat{a}_{VA} + \hat{a}_{VB}),$$

$$\hat{a}_3 = \frac{1}{\sqrt{2}}(-\hat{a}_{HA} + \hat{a}_{HB}), \quad \hat{a}_4 = \frac{1}{\sqrt{2}}(-\hat{a}_{VA} + \hat{a}_{VB}).$$

Polarization beam splitters allow one to separate photons with horizontal and vertical polarization and position of photon each group in a separate detector. In accordance with the photodetection theory (Soderholm et al. 2012), the probability of detecting n_1, n_2, n_3, n_4 photons on detectors 1, 2, 3, 4, respectively, is determined by the formula:

$$P_{n_1, n_2, n_3, n_4} = Tr\left(\hat{\Pi}_1^{(n_1)}\hat{\Pi}_2^{(n_2)}\hat{\Pi}_3^{(n_3)}\hat{\Pi}_4^{(n_4)}\hat{\rho}\right), \tag{3}$$

where $\hat{\rho}$ is the density operator of the light before the detection,

$$\hat{\Pi}_x^{(n)} =: \left| \frac{(\eta_x \hat{n}_x + N_x)^n}{n!} \exp(-\eta_x \hat{n}_x - N_x) \right|: \tag{4}$$

is the measurement operator for detector x , where η_x is the detector efficiency, \hat{n}_x is the photon number operator at the input of the detector x , means normal ordering, and N_x is the number of wrong counts related to the dark counts and the background radiation.

Model of the atmospheric influence

One of the main objectives of this work is to describe the passage of light through a turbulent atmosphere (sections A and B in the diagram in Figure 3). Similarly to the approach used by (Bohmann et al. 2016; Semenov, Vogel 2009; Vasylyev et al. 2016), who studied a similar problem, we consider the atmosphere as a system with damped oscillations.

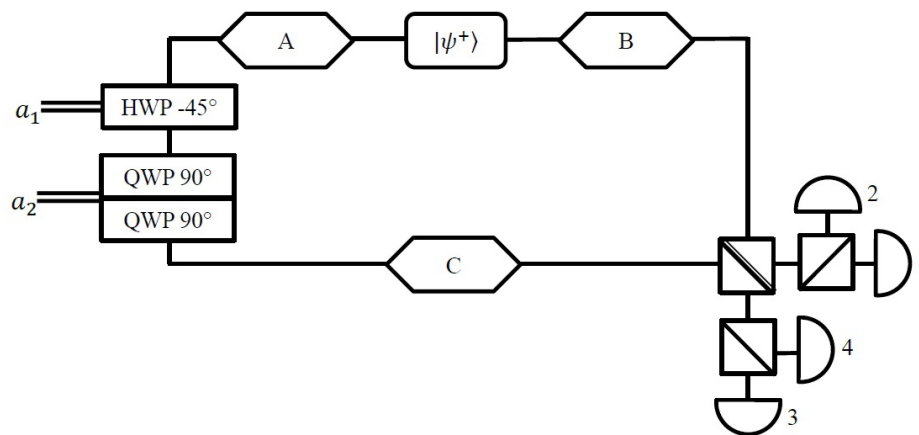


Fig. 3. Theoretical model of the device

The equations connecting the annihilation operators before and after passing through the atmosphere are as follows

$$\begin{aligned}\hat{a}_H^{out} &= T_H \hat{a}_H^{in} + T_{HV} \hat{a}_V^{in} + R_H \hat{c}_H^{in}, \\ \hat{a}_V^{out} &= T_V \hat{a}_V^{in} + T_{VH} \hat{a}_H^{in} + R_V \hat{c}_V^{in},\end{aligned}\tag{5}$$

where T_H and T_V are the transmission coefficients for the horizontal and the vertical modes, T_{HV} and T_{VH} are the depolarization coefficients, R_H and R_V are coefficients related to losses due to the reflection and the absorption described by operators \hat{c}_H^{in} and \hat{c}_V^{in} , respectively. It was shown by (Semenov, Vogel 2009) that the depolarizing effect of the atmosphere is very small. Hence, it is possible to assume that, $T_{HV} \approx 0$, $T_H \approx T_V \equiv T$. This allows one to simplify (5):

$$\hat{a}_H^{out} = T \hat{a}_H^{in} + R_H \hat{c}_H^{in}, \quad \hat{a}_V^{out} = T \hat{a}_V^{in} + R_V \hat{c}_V^{in}.\tag{6}$$

Normalization leads to the relation

$$|T|^2 + |R_{H(V)}|^2 = 1.\tag{7}$$

The atmosphere is random media so it can be considered as a quantum channel characterized by fluctuating transmission properties. Therefore, the turbulence can be modeled by introducing probability distribution function of transmission coefficient, which should correspond with turbulence condition. It was shown by (Gumberidze et al. 2016) that, depending on turbulence case, different functions would approximate the transmission coefficient distribution. We consider the case of strong turbulence only.

Model

Bell states transmission through atmosphere

We deal with the following initial state

$$|\psi^+\rangle = \frac{1}{\sqrt{2}} (|1001\rangle + |0110\rangle).\tag{8}$$

The density operator of the photons state $|\psi^+\rangle$ is

$$\hat{\rho}_{in} = |\psi^+\rangle \langle \psi^+|.$$

Let us calculate density operators after Alice's coding described by (2):

$$\hat{\rho}_{Alice}^{00} = \hat{\rho}_{in},\tag{9}$$

$$\hat{\rho}_{Alice}^{01} = \hat{\rho}_{\phi^+} = |\phi^+\rangle \langle \phi^+|,\tag{10}$$

$$\hat{\rho}_{Alice}^{10} = \hat{\rho}_{\psi^-} = |\psi^-\rangle \langle \psi^-|,\tag{11}$$

$$\hat{\rho}_{Alice}^{11} = \hat{\rho}_{\phi^-} = |\phi^-\rangle \langle \phi^-|.\tag{12}$$

To obtain the density operator for the state after the light transmission of paths A and B, we will use the approach of the input-output relations in terms of the Glauber–Sudarshan P-function. This approach was applied for deriving the output density matrices of the transmitted light in turbulent atmosphere by (Semenov, Vogel 2010).

Well-known Glauber–Sudarshan P-function is defined by determining the form of the density operator $\hat{\rho}$ in the basis of coherent states $\{|\alpha\rangle\}$:

$$\hat{\rho} = \int P(\alpha) |\alpha\rangle \langle \alpha| d^2\alpha.\tag{13}$$

The next formula for the P-function is more important for the practical calculations:

$$P(\alpha) = \frac{1}{\pi^2} \int_{-\infty}^{+\infty} \chi(\beta) \exp(\alpha\beta^* - \alpha^*\beta) d^2\beta. \quad (14)$$

Here, $\chi(\beta) = \text{Tr}[\hat{\rho} \exp(\hat{a}^+\beta) \exp(-\hat{a}\beta^*)]$ is the characteristic function; \hat{a} , \hat{a}^+ are the annihilation and creation operators.

Relations for the above functions between the input state and the transmitted state are given by the following expressions:

$$\hat{\rho}_{out} = \int P_{out}(\alpha) |\alpha\rangle\langle\alpha| d^2\alpha, \quad (15)$$

$$P_{out}(\alpha) = \frac{1}{T^2} P_{in}\left(\frac{\alpha}{T}\right), \quad (16)$$

$$\chi_{out}(\beta) = \chi_{in}(T\beta). \quad (17)$$

Formulas (13)–(17) allow one to derive the expression for the output density operator of the states (9)–(12) when the qubit coded by Alice is sent by path A and another qubit is sent by path B:

$$\begin{aligned} \hat{\rho}_{AB} &= (1-|T_A|^2)(1-|T_B|^2) \hat{\rho}_{vac} + \frac{1}{2}(1-|T_B|^2)|T_A|^2 \hat{\rho}_{H_A} + \frac{1}{2}(1-|T_B|^2)|T_A|^2 \hat{\rho}_{V_A} + \\ &+ \frac{1}{2}(1-|T_A|^2)|T_B|^2 \hat{\rho}_{H_B} + \frac{1}{2}(1-|T_A|^2)|T_B|^2 \hat{\rho}_{V_B} + |T_A|^2|T_B|^2 \hat{\rho}_{in}, \end{aligned}$$

$$\begin{aligned} \hat{\rho}_{AB} &= (1-|T_A|^2)(1-|T_B|^2) \hat{\rho}_{vac} + \frac{1}{2}(1-|T_B|^2)|T_A|^2 \hat{\rho}_{H_A} + \frac{1}{2}(1-|T_B|^2)|T_A|^2 \hat{\rho}_{V_A} + \\ &+ \frac{1}{2}(1-|T_A|^2)|T_B|^2 \hat{\rho}_{H_B} + \frac{1}{2}(1-|T_A|^2)|T_B|^2 \hat{\rho}_{V_B} + |T_A|^2|T_B|^2 \hat{\rho}_{\phi^+}, \end{aligned}$$

$$\begin{aligned} \hat{\rho}_{AB} &= (1-|T_A|^2)(1-|T_B|^2) \hat{\rho}_{vac} + \frac{1}{2}(1-|T_B|^2)|T_A|^2 \hat{\rho}_{H_A} + \frac{1}{2}(1-|T_B|^2)|T_A|^2 \hat{\rho}_{V_A} + \\ &+ \frac{1}{2}(1-|T_A|^2)|T_B|^2 \hat{\rho}_{H_B} + \frac{1}{2}(1-|T_A|^2)|T_B|^2 \hat{\rho}_{V_B} + |T_A|^2|T_B|^2 \hat{\rho}_{\psi^-}, \end{aligned}$$

$$\begin{aligned} \hat{\rho}_{AB} &= (1-|T_A|^2)(1-|T_B|^2) \hat{\rho}_{vac} + \frac{1}{2}(1-|T_B|^2)|T_A|^2 \hat{\rho}_{H_A} + \frac{1}{2}(1-|T_B|^2)|T_A|^2 \hat{\rho}_{V_A} + \\ &+ \frac{1}{2}(1-|T_A|^2)|T_B|^2 \hat{\rho}_{H_B} + \frac{1}{2}(1-|T_A|^2)|T_B|^2 \hat{\rho}_{V_B} + |T_A|^2|T_B|^2 \hat{\rho}_{\phi^-}, \end{aligned}$$

where $T_{A,B}$ are random transmission coefficients in the direction of the A(B) paths respectively; $\hat{\rho}_{vac}$ is the density operator of vacuum state, $\hat{\rho}_{H_{A,B}}$ and $\hat{\rho}_{V_{A,B}}$ are the density operators of one photon states, $\hat{\rho}_{in}$ is the density operator of the initial Bell state.

According to these results, it can be seen that either the zero-photon, or one of the eight different single-photon states, or a specific two-photon state, which depends only on the coding on the Alice's side, comes to the input of the beam splitter with the corresponding probabilities. For further calculation, it is necessary to express the annihilation operators of incoming modes through the outgoing operators:

$$\hat{a}_{H_A} = \frac{1}{\sqrt{2}}(\hat{a}_1 - \hat{a}_3), \quad (18)$$

$$\hat{a}_{V_A} = \frac{1}{\sqrt{2}}(\hat{a}_2 - \hat{a}_4), \quad (19)$$

$$\hat{a}_{H_B} = \frac{1}{\sqrt{2}}(\hat{a}_1 + \hat{a}_3), \quad (20)$$

$$\hat{a}_{V_B} = \frac{1}{\sqrt{2}}(\hat{a}_2 + \hat{a}_4). \quad (21)$$

The transformation of the single-photon states and the Bell states during the passage of the beam splitter is as follows:

$$|\gamma\rangle_{1D} = |1000\rangle = \hat{a}_{H_A}^\dagger |0000\rangle = (\hat{a}_1^\dagger - \hat{a}_3^\dagger) |0000\rangle = (|1\rangle_1 |0\rangle_2 |0\rangle_3 |0\rangle_4 - |0\rangle_1 |0\rangle_2 |1\rangle_3 |0\rangle_4), \quad (22)$$

$$|\gamma\rangle_{2D} = |0100\rangle = \hat{a}_{V_A}^\dagger |0000\rangle = (\hat{a}_2^\dagger - \hat{a}_4^\dagger) |0000\rangle = (|0\rangle_1 |1\rangle_2 |0\rangle_3 |0\rangle_4 - |0\rangle_1 |0\rangle_2 |0\rangle_3 |1\rangle_4), \quad (23)$$

$$|\gamma\rangle_{3D} = |0010\rangle = \hat{a}_{H_B}^\dagger |0000\rangle = (\hat{a}_1^\dagger + \hat{a}_3^\dagger) |0000\rangle = (|1\rangle_1 |0\rangle_2 |0\rangle_3 |0\rangle_4 + |0\rangle_1 |0\rangle_2 |1\rangle_3 |0\rangle_4), \quad (24)$$

$$|\gamma\rangle_{4D} = |0001\rangle = \hat{a}_{V_B}^\dagger |0000\rangle = (\hat{a}_2^\dagger + \hat{a}_4^\dagger) |0000\rangle = (|0\rangle_1 |1\rangle_2 |0\rangle_3 |0\rangle_4 + |0\rangle_1 |0\rangle_2 |0\rangle_3 |1\rangle_4), \quad (25)$$

$$|\psi^+\rangle_D = \frac{1}{\sqrt{2}}(|1001\rangle + |0110\rangle) = \frac{1}{\sqrt{2}}(\hat{a}_{H_A}^\dagger \hat{a}_{V_B}^\dagger + \hat{a}_{V_A}^\dagger \hat{a}_{H_B}^\dagger) |0000\rangle = \frac{1}{2\sqrt{2}}((\hat{a}_1^\dagger - \hat{a}_3^\dagger)(\hat{a}_2^\dagger + \hat{a}_4^\dagger) + (\hat{a}_2^\dagger - \hat{a}_4^\dagger)(\hat{a}_1^\dagger + \hat{a}_3^\dagger)) |0000\rangle = \quad (26)$$

$$\frac{1}{2\sqrt{2}}(2\hat{a}_1^\dagger \hat{a}_2^\dagger - 2\hat{a}_3^\dagger \hat{a}_4^\dagger) |0000\rangle = \frac{1}{\sqrt{2}}(|1\rangle_1 |1\rangle_2 |0\rangle_3 |0\rangle_4 - |0\rangle_1 |0\rangle_2 |1\rangle_3 |1\rangle_4),$$

$$|\phi^+\rangle_D = \frac{1}{\sqrt{2}}(|0101\rangle + |1010\rangle) = \frac{1}{\sqrt{2}}(\hat{a}_{H_A}^\dagger \hat{a}_{H_B}^\dagger + \hat{a}_{V_A}^\dagger \hat{a}_{V_B}^\dagger) |0000\rangle =$$

$$\frac{1}{2\sqrt{2}}((\hat{a}_1^\dagger - \hat{a}_3^\dagger)(\hat{a}_1^\dagger + \hat{a}_3^\dagger) + (\hat{a}_2^\dagger - \hat{a}_4^\dagger)(\hat{a}_2^\dagger + \hat{a}_4^\dagger)) |0000\rangle = \quad (27)$$

$$\frac{1}{2\sqrt{2}}((\hat{a}_1^\dagger)^2 - (\hat{a}_3^\dagger)^2 + (\hat{a}_2^\dagger)^2 - (\hat{a}_4^\dagger)^2) |0000\rangle =$$

$$\frac{1}{2}(|2\rangle_1 |0\rangle_2 |0\rangle_3 |0\rangle_4 + |0\rangle_1 |2\rangle_2 |0\rangle_3 |0\rangle_4 - |0\rangle_1 |0\rangle_2 |2\rangle_3 |0\rangle_4 - |0\rangle_1 |0\rangle_2 |0\rangle_3 |2\rangle_4)$$

Analogously, for states $|\psi^-\rangle$ and $|\phi^-\rangle$:

$$|\psi^-\rangle_D = \frac{1}{\sqrt{2}}(|1\rangle_1 |0\rangle_2 |0\rangle_3 |1\rangle_4 - |0\rangle_1 |1\rangle_2 |1\rangle_3 |0\rangle_4). \quad (28)$$

$$|\phi^-\rangle_D = \frac{1}{2}(|2\rangle_1 |0\rangle_2 |0\rangle_3 |0\rangle_4 - |0\rangle_1 |2\rangle_2 |0\rangle_3 |0\rangle_4 - |0\rangle_1 |0\rangle_2 |2\rangle_3 |0\rangle_4 + |0\rangle_1 |0\rangle_2 |0\rangle_3 |2\rangle_4) \quad (29)$$

Thus, the density operator for photons before the detection has the form:

$$\hat{P}_{out} = P_{vac} \hat{P}_{(vac)} + P_A \hat{P}_{(A)} + P_B \hat{P}_{(B)} + P_{Bell} \hat{P}_{(Bell)}, \quad (30)$$

where the transmission probabilities of different numbers of photons are as follows

$$p_{vac} = (1 - |T_A|^2)(1 - |T_B|^2), \tag{31}$$

$$p_A = p_{H_A} = p_{V_A} = \frac{1}{2}|T_A|^2(1 - |T_B|^2), \tag{32}$$

$$p_B = p_{H_B} = p_{V_B} = \frac{1}{2}|T_B|^2(1 - |T_A|^2), \tag{33}$$

$$p_2 = |T_A|^2|T_B|^2. \tag{34}$$

Here $\hat{\rho}_{(vac)}$ is a vacuum state,

$$\hat{\rho}_{(A)} = |\gamma\rangle_{1D}\langle\gamma| + |\gamma\rangle_{2D}\langle\gamma|,$$

$$\hat{\rho}_{(B)} = |\gamma\rangle_{3D}\langle\gamma| + |\gamma\rangle_{4D}\langle\gamma|$$

are single-photon density operators observed by one detector, $\hat{\rho}_{(Bell)}$ is a two-photon state of different forms depending on the sent qubits: $\hat{\rho}_{00} = |\psi^+\rangle_D\langle\psi^+|$, or $\hat{\rho}_{01} = |\varphi^+\rangle_D\langle\varphi^+|$, or $\hat{\rho}_{10} = |\psi^-\rangle_D\langle\psi^-|$, or $\hat{\rho}_{11} = |\varphi^-\rangle_D\langle\varphi^-|$.

Bell states detection

As in (30) one term only depends on sent qubits ($\hat{\rho}_{Bell}$), one should take the following expressions (based on (26)-(29)) as probabilities of distinguishing qubit pairs:

$$P_{00} = Tr(\hat{\Pi}_1^{(1)}\hat{\Pi}_2^{(1)}\hat{\Pi}_3^{(0)}\hat{\Pi}_4^{(0)}\hat{\rho}) + Tr(\hat{\Pi}_1^{(0)}\hat{\Pi}_2^{(0)}\hat{\Pi}_3^{(1)}\hat{\Pi}_4^{(1)}\hat{\rho}), \tag{35}$$

$$P_{10} = Tr(\hat{\Pi}_1^{(1)}\hat{\Pi}_2^{(0)}\hat{\Pi}_3^{(0)}\hat{\Pi}_4^{(1)}\hat{\rho}) + Tr(\hat{\Pi}_1^{(0)}\hat{\Pi}_2^{(1)}\hat{\Pi}_3^{(1)}\hat{\Pi}_4^{(0)}\hat{\rho}), \tag{36}$$

$$P_{01} = P_{11} = \frac{1}{2} (Tr(\hat{\Pi}_1^{(2)}\hat{\Pi}_2^{(0)}\hat{\Pi}_3^{(0)}\hat{\Pi}_4^{(0)}\hat{\rho}) + Tr(\hat{\Pi}_1^{(0)}\hat{\Pi}_2^{(2)}\hat{\Pi}_3^{(0)}\hat{\Pi}_4^{(0)}\hat{\rho})) + Tr(\hat{\Pi}_1^{(0)}\hat{\Pi}_2^{(0)}\hat{\Pi}_3^{(2)}\hat{\Pi}_4^{(0)}\hat{\rho}) + Tr(\hat{\Pi}_1^{(0)}\hat{\Pi}_2^{(0)}\hat{\Pi}_3^{(0)}\hat{\Pi}_4^{(2)}\hat{\rho}). \tag{37}$$

The general form of the measurement operator is given in (4). Let us calculate the images of different states under the action of this operator.

$$\begin{aligned} \hat{\Pi}_x^{(0)}|0\rangle_x\langle 0| &= e^{(-\eta_x\hat{n}_x - N_x)}|0\rangle_x\langle 0| = \\ e^{-N_x} \left(\sum_{k=0}^{\infty} \frac{(-1)^k}{k!} \eta_x^k \hat{n}_x^k \right) |0\rangle_x\langle 0| &= \\ = e^{-N_x} |0\rangle_x\langle 0|, \end{aligned} \tag{38}$$

$$\begin{aligned} \hat{\Pi}_x^{(0)}|1\rangle_x\langle 1| &= e^{-N_x} \left(1 - \eta_x\hat{n}_x + \sum_{k=2}^{\infty} \frac{(-1)^k}{k!} \eta_x^k \hat{n}_x^k \right) |1\rangle_x\langle 1| = \\ (1 - \eta_x) e^{-N_x} |1\rangle_x\langle 1|, \end{aligned} \tag{39}$$

$$\begin{aligned} \hat{\Pi}_x^{(0)}|2\rangle_x\langle 2| &= e^{-N_x} \left(1 - \eta_x\hat{n}_x + \frac{1}{2}\eta_x^2\hat{n}_x^2 + \sum_{k=3}^{\infty} \frac{(-1)^k}{k!} \eta_x^k \hat{n}_x^k \right) |2\rangle_x\langle 2| = \\ (1 - 2\eta_x + \eta_x^2) e^{-N_x} |2\rangle_x\langle 2| = (1 - \eta_x)^2 e^{-N_x} |2\rangle_x\langle 2|, \end{aligned} \tag{40}$$

$$\begin{aligned} \hat{\Pi}_x^{(1)}|0\rangle_x\langle 0| &= \left((\eta_x \hat{n}_x + N_x) e^{(-\eta_x \hat{n}_x - N_x)} \right) |0\rangle_x\langle 0| = \\ e^{-N_x} \left((\eta_x \hat{n}_x + N_x) \left(1 + \sum_{k=1}^{\infty} \frac{(-1)^k}{k!} \eta_x^k \hat{n}_x^k \right) \right) |0\rangle_x\langle 0| &= \\ N_x e^{-N_x} |0\rangle_x\langle 0|, \end{aligned} \quad (41)$$

$$\begin{aligned} \hat{\Pi}_x^{(1)}|1\rangle_x\langle 1| &= e^{-N_x} \left((\eta_x \hat{n}_x + N_x) \left(1 - \eta_x \hat{n}_x + \sum_{k=2}^{\infty} \frac{(-1)^k}{k!} \eta_x^k \hat{n}_x^k \right) \right) \\ |1\rangle_x\langle 1| &= (\eta_x + N_x (1 - \eta_x)) e^{-N_x} |1\rangle_x\langle 1|, \end{aligned} \quad (42)$$

$$\begin{aligned} \hat{\Pi}_x^{(1)}|2\rangle_x\langle 2| &= e^{-N_x} (\eta_x \hat{n}_x + N_x) \left(1 - \eta_x \hat{n}_x + \frac{1}{2} \eta_x^2 \hat{n}_x^2 + \right. \\ \left. \sum_{k=3}^{\infty} \frac{(-1)^k}{k!} \eta_x^k \hat{n}_x^k \right) |2\rangle_x\langle 2| &= (2\eta_x - 2\eta_x^2 + N_x (1 - 2\eta_x + \eta_x^2)) \\ e^{-N_x} |2\rangle_x\langle 2| &= (1 - \eta_x) (2\eta_x + N_x (1 - \eta_x)) e^{-N_x} |2\rangle_x\langle 2|, \end{aligned} \quad (43)$$

$$\begin{aligned} \hat{\Pi}_x^{(2)}|0\rangle_x\langle 0| &= \left(\frac{1}{2} (\eta_x^2 \hat{n}_x^2 + 2N_x \eta_x \hat{n}_x + N_x^2) e^{(-\eta_x \hat{n}_x - N_x)} \right) |0\rangle_x\langle 0| = \\ \frac{1}{2} e^{-N_x} \left((\eta_x^2 \hat{n}_x^2 + 2N_x \eta_x \hat{n}_x + N_x^2) \left(1 + \sum_{k=1}^{\infty} \frac{(-1)^k}{k!} \eta_x^k \hat{n}_x^k \right) \right) |0\rangle_x\langle 0| &= \\ \frac{1}{2} N_x^2 e^{-N_x} |0\rangle_x\langle 0|, \end{aligned} \quad (44)$$

$$\begin{aligned} \hat{\Pi}_x^{(2)}|1\rangle_x\langle 1| &= \frac{1}{2} e^{-N_x} \left((\eta_x^2 \hat{n}_x^2 + 2N_x \eta_x \hat{n}_x + N_x^2) (1 - \eta_x \hat{n}_x + \right. \\ \left. \sum_{k=2}^{\infty} \frac{(-1)^k}{k!} \eta_x^k \hat{n}_x^k) \right) |1\rangle_x\langle 1| &= \frac{1}{2} (2N_x \eta_x + N_x^2 (1 - \eta_x)) e^{-N_x} |1\rangle_x\langle 1| = \\ N_x \left(\eta_x + \frac{1}{2} N_x (1 - \eta_x) \right) e^{-N_x} |1\rangle_x\langle 1|, \end{aligned} \quad (45)$$

$$\begin{aligned} \hat{\Pi}_x^{(2)}|2\rangle_x\langle 2| &= \frac{1}{2} e^{-N_x} \left((\eta_x^2 \hat{n}_x^2 + 2N_x \eta_x \hat{n}_x + N_x^2) (1 - \eta_x \hat{n}_x + \frac{1}{2} \eta_x^2 \hat{n}_x^2 + \right. \\ \left. + N_x^2 (1 - \eta_x)^2) e^{-N_x} |2\rangle_x\langle 2| &= \left(\eta_x^2 + 2\eta_x N_x (1 - \eta_x) + \frac{1}{2} N_x^2 (1 - \eta_x)^2 \right) e^{-N_x} |2\rangle_x\langle 2|. \end{aligned} \quad (46)$$

Let us consider the situation with identical detectors and identical values of the background noise. We will reveal the dependencies between the model parameters and the probabilities (35)–(37). In this case $\eta_x = \eta_D$ and $N_x = N_D$ for all $x \in \{1, 2, 3, 4\}$.

Trace is a linear operator. Correspondingly, one can calculate the probabilities separately for density operators $\hat{\rho}_{vac}, \hat{\rho}_A, \hat{\rho}_B, \hat{\rho}_{Bell}$ and obtain the result as a linear combination with coefficients (31)–(34). Particularly, for $\hat{\rho}_{(vac)}$ one has:

$$P_{00}(\hat{\rho}_{vac}) = P_{10}(\hat{\rho}_{vac}) = 2 \text{Tr} \left(N_D^2 e^{-4N_D} \hat{\rho}_{vac} \right) = 2 N_D^2 e^{-4N_D}, \quad (47)$$

$$P_{01}(\hat{\rho}_{vac}) = P_{11}(\hat{\rho}_{vac}) = \frac{1}{2} \cdot 4 \text{Tr} \left(\frac{1}{2} N_D^2 e^{-4N_D} \hat{\rho}_{vac} \right) = N_D^2 e^{-4N_D}. \quad (48)$$

Before calculating $\hat{\rho}_A, \hat{\rho}_B$, let us consider

$$Tr\left(\hat{\Pi}_1^1 \hat{\Pi}_2^1 \hat{\Pi}_3^0 \hat{\Pi}_4^0 \hat{\rho}_A\right)$$

and

$$Tr\left(\hat{\Pi}_1^2 \hat{\Pi}_2^0 \hat{\Pi}_3^0 \hat{\Pi}_4^0 \hat{\rho}_A\right).$$

$$\begin{aligned} Tr\left(\hat{\Pi}_1^1 \hat{\Pi}_2^1 \hat{\Pi}_3^0 \hat{\Pi}_4^0 \hat{\rho}_A\right) &= Tr\left(\hat{\Pi}_1^1 \hat{\Pi}_2^1 \hat{\Pi}_3^0 \hat{\Pi}_4^0 (|\gamma\rangle_{1D} \langle \gamma|_{1D} + |\gamma\rangle_{2D} \langle \gamma|_{2D})\right) = \\ &= Tr\left(\hat{\Pi}_1^1 \hat{\Pi}_2^1 \hat{\Pi}_3^0 \hat{\Pi}_4^0 (|1000\rangle \langle 1000| - |0010\rangle \langle 1000| - |1000\rangle \langle 0010| + |0010\rangle \langle 0010| + \right. \\ &\quad \left. + |0100\rangle \langle 0100| - |0100\rangle \langle 0001| - |0001\rangle \langle 0100| + |0001\rangle \langle 0001|\right), \end{aligned}$$

$$\begin{aligned} Tr\left(\hat{\Pi}_1^1 \hat{\Pi}_2^1 \hat{\Pi}_3^0 \hat{\Pi}_4^0 \hat{\rho}_B\right) &= Tr\left(\hat{\Pi}_1^1 \hat{\Pi}_2^1 \hat{\Pi}_3^0 \hat{\Pi}_4^0 (|\gamma\rangle_{3D} \langle \gamma|_{3D} + |\gamma\rangle_{4D} \langle \gamma|_{4D})\right) = \\ &= Tr\left(\hat{\Pi}_1^1 \hat{\Pi}_2^1 \hat{\Pi}_3^0 \hat{\Pi}_4^0 (|1000\rangle \langle 1000| + |0010\rangle \langle 1000| + |1000\rangle \langle 0010| + |0010\rangle \langle 0010| + \right. \\ &\quad \left. + |0100\rangle \langle 0100| + |0100\rangle \langle 0001| + |0001\rangle \langle 0100| + |0001\rangle \langle 0001|\right). \end{aligned}$$

To find a trace, one is interested in diagonal elements only. Hence,

$$Tr\left(\hat{\Pi}_1^{x1} \hat{\Pi}_2^{x2} \hat{\Pi}_3^{x3} \hat{\Pi}_4^{x4} \hat{\rho}_A\right) = Tr\left(\hat{\Pi}_1^{x1} \hat{\Pi}_2^{x2} \hat{\Pi}_3^{x3} \hat{\Pi}_4^{x4} \hat{\rho}_B\right).$$

Consequently,

$$\begin{aligned} Tr\left(\hat{\Pi}_1^1 \hat{\Pi}_2^1 \hat{\Pi}_3^0 \hat{\Pi}_4^0 \hat{\rho}_A\right) &= Tr\left(\hat{\Pi}_1^1 \hat{\Pi}_2^1 \hat{\Pi}_3^0 \hat{\Pi}_4^0 \hat{\rho}_B\right) = 2(\eta_D + N_D(1 - \eta_D)) N_D e^{-4N_D} + \\ &2(1 - \eta_D) N_D^2 e^{-4N_D} = 2N_D \left((\eta_D + 2N_D(1 - \eta_D)) \right) e^{-4N_D}, \end{aligned} \tag{49}$$

$$\begin{aligned} Tr\left(\hat{\Pi}_1^2 \hat{\Pi}_2^0 \hat{\Pi}_3^0 \hat{\Pi}_4^0 \hat{\rho}_A\right) &= Tr\left(\hat{\Pi}_1^2 \hat{\Pi}_2^0 \hat{\Pi}_3^0 \hat{\Pi}_4^0 \hat{\rho}_B\right) = \left(\eta_D + \frac{1}{2} N_D (1 - \eta_D) \right) N_D e^{-4N_D} + \\ &+ \frac{3}{2} (1 - \eta_D) N_D^2 e^{-4N_D} = N_D \left((\eta_D + 2N_D(1 - \eta_D)) \right) e^{-4N_D}. \end{aligned} \tag{50}$$

Using (49) and (50), one obtains the probabilities for the density operator $\hat{\rho}_A, \hat{\rho}_B$:

$$P_{00}(\hat{\rho}_A) = P_{00}(\hat{\rho}_B) = P_{10}(\hat{\rho}_A) = P_{10}(\hat{\rho}_B) = 4N_D \left((\eta_D + 2N_D(1 - \eta_D)) \right) e^{-4N_D}, \tag{51}$$

$$P_{01}(\hat{\rho}_A) = P_{01}(\hat{\rho}_B) = P_{11}(\hat{\rho}_A) = P_{11}(\hat{\rho}_B) = 2N_D \left((\eta_D + 2N_D(1 - \eta_D)) \right) e^{-4N_D}. \tag{52}$$

Let us calculate the probabilities for the density operator $\hat{\rho}_{Belb}$, which takes different forms for different Alice's coding: $\hat{\rho}_{00}, \hat{\rho}_{01}, \hat{\rho}_{10}, \hat{\rho}_{11}$:

$$\begin{aligned} P_{00}(\hat{\rho}_{00}) &= \left(\frac{1}{2} (\eta_D + N_D(1 - \eta_D))^2 e^{-4N_D} + \frac{1}{2} N_D^2 (1 - \eta_D)^2 e^{-4N_D} \right) + \\ &\left(\frac{1}{2} N_D^2 (1 - \eta_D)^2 e^{-4N_D} + \frac{1}{2} (\eta_D + N_D(1 - \eta_D))^2 e^{-4N_D} \right) = \\ &(\eta_D^2 + 2N_D(1 - \eta_D)(\eta_D + N_D(1 - \eta_D))) e^{-4N_D}, \end{aligned} \tag{53}$$

$$P_{10}(\hat{\rho}_{00}) = 4 \left(\frac{1}{2} (\eta_D + N_D (1 - \eta_D)) (1 - \eta_D) N_D e^{-4N_D} \right) = \tag{54}$$

$$2N_D (1 - \eta_D) (\eta_D + N_D (1 - \eta_D)) e^{-4N_D},$$

$$P_{01}(\hat{\rho}_{00}) = P_{11}(\hat{\rho}_{00}) = \frac{1}{2} \cdot 4 (N_D \left(\eta_D + \frac{1}{2} N_D (1 - \eta_D) \right) (1 - \eta_D) e^{-4N_D} + \tag{55}$$

$$\frac{1}{2} N_D^2 (1 - \eta_D)^2 e^{-4N_D}) = 2N_D (1 - \eta_D) (\eta_D + N_D (1 - \eta_D)) e^{-4N_D},$$

$$P_{00}(\hat{\rho}_{10}) = 4 \left(\frac{1}{2} (\eta_D + N_D (1 - \eta_D)) (1 - \eta_D) N_D e^{-4N_D} \right) = \tag{56}$$

$$2N_D (1 - \eta_D) (\eta_D + N_D (1 - \eta_D)) e^{-4N_D},$$

$$P_{10}(\hat{\rho}_{10}) = \left(\frac{1}{2} (\eta_D + N_D (1 - \eta_D))^2 e^{-4N_D} + \frac{1}{2} N_D^2 (1 - \eta_D)^2 e^{-4N_D} \right) + \tag{57}$$

$$\left(\frac{1}{2} N_D^2 (1 - \eta_D)^2 e^{-4N_D} + \frac{1}{2} (\eta_D + N_D (1 - \eta_D))^2 e^{-4N_D} \right) =$$

$$(\eta_D^2 + 2N_D (1 - \eta_D) (\eta_D + N_D (1 - \eta_D))) e^{-4N_D},$$

$$P_{01}(\hat{\rho}_{10}) = P_{11}(\hat{\rho}_{10}) = \frac{1}{2} \cdot 4 (N_D \left(\eta_D + \frac{1}{2} N_D (1 - \eta_D) \right) (1 - \eta_D) e^{-4N_D} + \tag{58}$$

$$\frac{1}{2} N_D^2 (1 - \eta_D)^2 e^{-4N_D}) = 2N_D (1 - \eta_D) (\eta_D + N_D (1 - \eta_D)) e^{-4N_D},$$

$$P_{00}(\hat{\rho}_{01}) = P_{00}(\hat{\rho}_{11}) = P_{10}(\hat{\rho}_{01}) = P_{10}(\hat{\rho}_{11}) = \tag{59}$$

$$4 \cdot \frac{1}{4} \left((1 - \eta_D) (2\eta_D + N_D (1 - \eta_D)) N_D e^{-4N_D} + N_D^2 (1 - \eta_D)^2 e^{-4N_D} \right) =$$

$$2N_D (1 - \eta_D) (\eta_D + N_D (1 - \eta_D)) e^{-4N_D},$$

$$P_{01}(\hat{\rho}_{01}) = P_{11}(\hat{\rho}_{01}) = P_{01}(\hat{\rho}_{11}) = P_{11}(\hat{\rho}_{11}) = \frac{1}{2} \cdot 4 \cdot \frac{1}{4} ((\eta_D^2 + \tag{60}$$

$$2\eta_D N_D (1 - \eta_D) + \frac{1}{2} N_D^2 (1 - \eta_D)^2) e^{-4N_D} + 3 \cdot \frac{1}{2} N_D^2 (1 - \eta_D)^2 e^{-4N_D} =$$

$$\frac{1}{2} (\eta_D^2 + 2N_D (1 - \eta_D) (\eta_D + N_D (1 - \eta_D))) e^{-4N_D}.$$

It is necessary to perform a post-selection of obtained results. In fact, it means to make a normalization of obtained values. We calculate sums of probabilities:

$$S_{00|10} = p_{vac} (8N_D^2 e^{-4N_D}) + (p_A + p_B) (16N_D (\eta_D + 2N_D (1 - \eta_D))) e^{-4N_D} + \tag{61}$$

$$+ p_{Bell} (8N_D (1 - \eta_D) (\eta_D + N_D (1 - \eta_D)) + \eta_D^2) e^{-4N_D}$$

$$S_{01|11} = p_{vac} (4N_D^2 e^{-4N_D}) + (p_A + p_B) (8N_D (\eta_D + 2N_D (1 - \eta_D))) e^{-4N_D} + \tag{62}$$

$$+ p_{Bell} (6N_D (1 - \eta_D) (\eta_D + N_D (1 - \eta_D)) + \eta_D^2) e^{-4N_D}$$

Then, (51)–(62) give one the following values of the probabilities in question:

$$P_{00 \rightarrow 00} = P_{10 \rightarrow 10} = \frac{2p_{vac}N_D^2 + 4(p_A + p_B)(N_D(\eta_D + 2N_D(1-\eta_D))) + p_{Bell}(2N_D(1-\eta_D)(\eta_D + N_D(1-\eta_D))) + 8p_{vac}N_D^2 + 16(p_A + p_B)(N_D(\eta_D + 2N_D(1-\eta_D))) + p_{Bell}(8N_D(1-\eta_D)(\eta_D + N_D(1-\eta_D))) + \eta_D^2}{8p_{vac}N_D^2 + 16(p_A + p_B)(N_D(\eta_D + 2N_D(1-\eta_D))) + p_{Bell}(8N_D(1-\eta_D)(\eta_D + N_D(1-\eta_D))) + \eta_D^2} \quad (63)$$

$$P_{00 \rightarrow 10} = P_{10 \rightarrow 00} = \frac{2p_{vac}N_D^2 + 4(p_A + p_B)(N_D(\eta_D + 2N_D(1-\eta_D))) + p_{Bell}(2N_D(1-\eta_D)(\eta_D + N_D(1-\eta_D)))}{8p_{vac}N_D^2 + 16(p_A + p_B)(N_D(\eta_D + 2N_D(1-\eta_D))) + p_{Bell}(8N_D(1-\eta_D)(\eta_D + N_D(1-\eta_D))) + \eta_D^2} \quad (64)$$

$$P_{01 \rightarrow 00} = P_{11 \rightarrow 00} = P_{01 \rightarrow 10} = P_{11 \rightarrow 10} = \frac{2p_{vac}N_D^2 + 4(p_A + p_B)(N_D(\eta_D + 2N_D(1-\eta_D))) + p_{Bell}(2N_D(1-\eta_D)(\eta_D + N_D(1-\eta_D)))}{8p_{vac}N_D^2 + 16(p_A + p_B)(N_D(\eta_D + 2N_D(1-\eta_D))) + p_{Bell}(8N_D(1-\eta_D)(\eta_D + N_D(1-\eta_D))) + \eta_D^2} \quad (65)$$

$$P_{00 \rightarrow 01} = P_{00 \rightarrow 11} = P_{10 \rightarrow 01} = P_{10 \rightarrow 11} = \frac{p_{vac}N_D^2 + 2(p_A + p_B)(N_D(\eta_D + 2N_D(1-\eta_D))) + p_{Bell}(2N_D(1-\eta_D)(\eta_D + N_D(1-\eta_D)))}{4p_{vac}N_D^2 + 8(p_A + p_B)(N_D(\eta_D + 2N_D(1-\eta_D))) + p_{Bell}(6N_D(1-\eta_D)(\eta_D + N_D(1-\eta_D))) + \eta_D^2} \quad (66)$$

$$P_{01 \rightarrow 01} = P_{11 \rightarrow 11} = P_{01 \rightarrow 11} = P_{11 \rightarrow 01} = \frac{p_{vac}N_D^2 + 2(p_A + p_B)(N_D(\eta_D + 2N_D(1-\eta_D))) + p_{Bell}\left(\frac{1}{2}\eta_D^2 + N_D(1-\eta_D)(\eta_D + N_D(1-\eta_D))\right)}{4p_{vac}N_D^2 + 8(p_A + p_B)(N_D(\eta_D + 2N_D(1-\eta_D))) + p_{Bell}(6N_D(1-\eta_D)(\eta_D + N_D(1-\eta_D))) + \eta_D^2} \quad (67)$$

where $P_{a_1a_2 \rightarrow b_1b_2}$ means that bits a_1a_2 are encoded by Alice and bits b_1b_2 are distinguished by Bob.

These probabilities were calculated numerically. We suppose that the time interval when Alice was coding her qubit is so small, that one can assume that qubits were sent to Bob at the same time and went through the same path. Hence, one can simply set $|T_A|^2 = |T_B|^2 = \eta_{atm}$, where η_{atm} is the fluctuating atmospheric efficiency, which is a random characteristic. In accordance with the (Gumberidze et al. 2016) the efficiency distribution could be described by lognormal distribution in strong turbulence conditions:

$$f(\eta_{atm}) = \frac{1}{\sqrt{2\pi}\sigma\eta_{atm}} \exp\left(-\frac{1}{2}\left(\frac{\ln\eta_{atm} + \bar{\theta}}{\sigma}\right)^2\right), \quad (68)$$

where $\bar{\theta} = -\ln\eta_{atm}$ characterizes the mean atmospheric losses, σ (the variance of $\theta = -\ln\eta_{atm}$) characterizes the atmosphere turbulence. This distribution can be applied only for $\sigma = \bar{\theta}$. We used the data from (Semenov, Vogel 2010) for calculations.

Discussion

So, what is the meaning of Expressions (63)–(67)? Firstly, Expression (67) shows that in one case the transmitted pair of bits is recognized correctly, and in the second it is incorrect, and these cases occur with equal probability. That is, this model has no way to distinguish pairs of bits 01 and 11.

Secondly, for every event that did not save the result (except (67)), the probability is a multiple of N_D . This means that if it is possible to reduce this indicator to zero, then this model will ideally implement the superdense coding algorithm, with the exception of the indistinguishability of bits 01 and 11. This can be seen in the graph below (Figure 4).

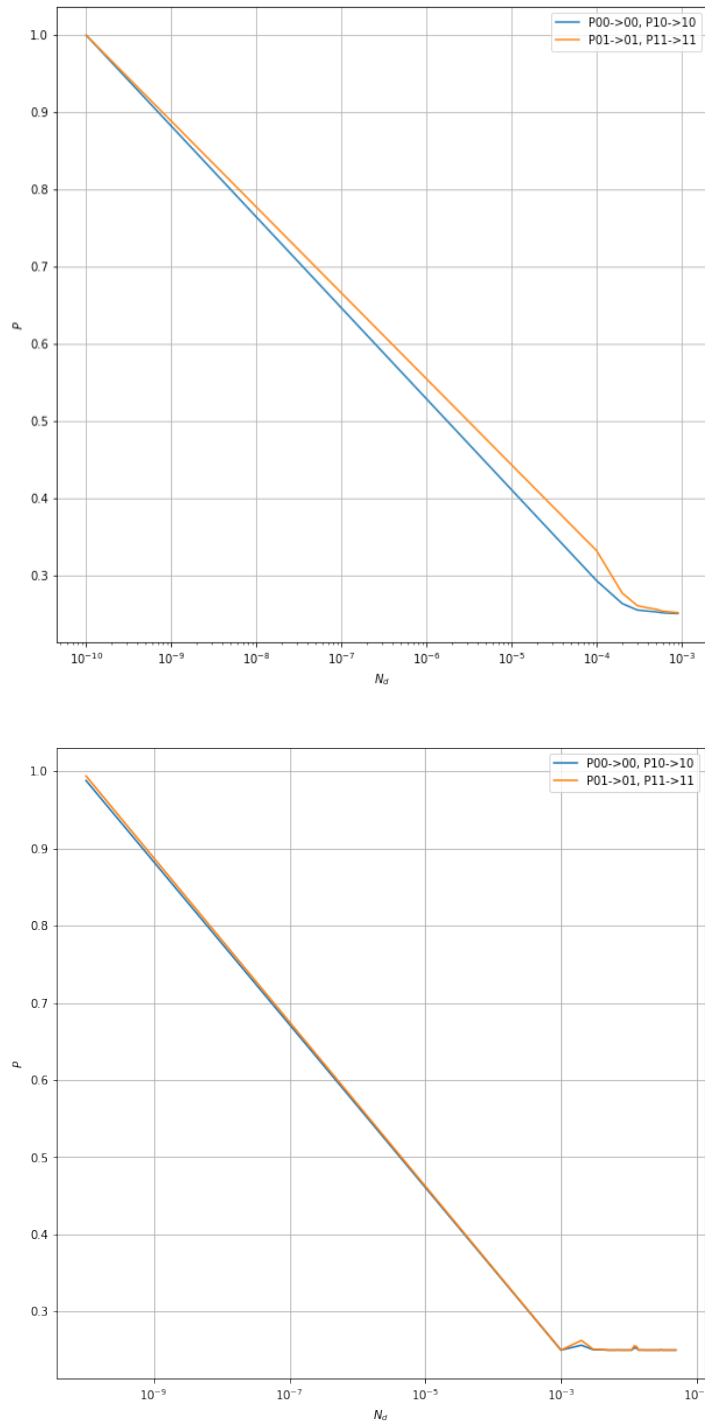


Fig. 4. Probability of correct recognition via the mean value of levels of the dark counts N_D ; the detection efficiency $\eta_D = 0.25$, the mean atmospheric losses are $\bar{\theta} = 7.36$, turbulence parameter: left: $\sigma = 0.1$, right: $\sigma = 2$

To analyze the results, it is important to understand that the minimum probability of correct operation of the algorithm is $1/3$ and $1/6$. Fixing one of the events (35)–(37) on the detectors, we understand which pair of bits was sent. In the worst case, events happen randomly, and as a result, we actually guess the forwarded bits, and the probability that we will guess is $1/3$ for bits 00|10 and $1/6$ for bits 01|11.

The graphs in Figures 4 and 5 show the dependencies of correct recognition on the number of dark counts for different values of the turbulence parameter. The values of atmospheric efficiency were generated randomly in accordance with the lognormal probability distribution. Figure 4 shows that adequate results of the algorithm (about 80 per cent recognition of bits 00|10) are obtained at $N_D \approx 10^{-8}$. But even about $N_D \approx 2 \cdot 10^{-6}$, the probabilities of correct recognition are close to random. We can also see that the

more we increase the value σ , the more different are the results (Figure 5). So when the turbulence instability is higher, the results may be less predictable.

Analyzing the influence of the detectors efficiency η_D , one obtains the following dependence (Fig. 5).

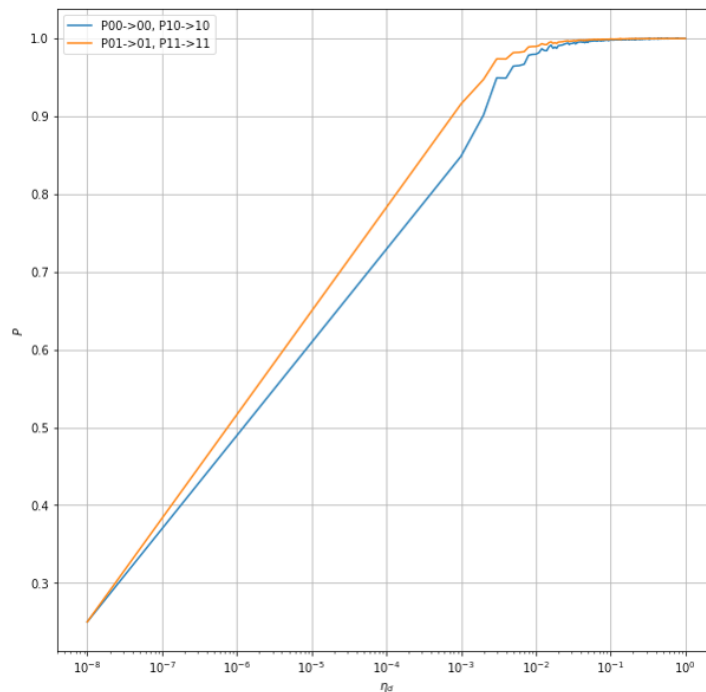


Fig. 5. Probability of correct recognition via the detectors efficiency η_D , $\sigma = 0.1$, $N_D = 10^{-8}$, the mean atmospheric losses are $\bar{\theta} = 7.36$

It follows from the graph that the recognition errors are small enough if detectors efficiency exceeds the value of about 10^{-3} .

Summarizing the results, one can mention that for the suggested theoretical model of a quantum channel for the implementation of the superdense coding quantum algorithm, the most important factors include the turbulence instability, detectors efficiency and the mean level of noise counts caused by the background radiation and the dark counts.

Conflict of interest

The authors declare that there is no conflict of interest, either existing or potential.

Authors contribution

The authors have made an equal contribution to the paper.

References

- Adam, I. A., Yashin, D. A., Kargina, D. A., Nasedkina, B. A. (2022) Comparison of Gaussian and vortex beams in free-space QKD with phase encoding in turbulent atmosphere. *Nanosystems: Physics, Chemistry, Mathematics*, 13 (4), 392–403. <https://doi.org/10.17586/2220-8054-2022-13-4-392-403> (In English)
- Bennett, C. H., Wiesner, S. J. (1992) Communication via one- and two-particle operators on Einstein-Podolsky-Rosen states. *Physical Review Letters*, 69 (20), article 2881. <https://doi.org/10.1103/PhysRevLett.69.2881> (In English)
- Bohmann, M., Semenov, A. A., Sperling, J., Vogel, W. (2016) Gaussian entanglement in the turbulent atmosphere. *Physical Review A*, 94 (1), article 010302(R). <https://doi.org/10.1103/PhysRevA.94.010302> (In English)
- Dong, R., Lassen, M. O., Heersink, J. et al. (2008) Experimental entanglement distillation of mesoscopic quantum states. *Nature Physics*, 4 (12), 919–923. <https://doi.org/10.1038/nphys1112> (In English)

- Elser, D., Bartley, T., Heim, B. et al. (2009) Feasibility of free space quantum key distribution with coherent polarization states. *New Journal of Physics*, 11, article 045014. <https://doi.org/10.1088/1367-2630/11/4/045014> (In English)
- Faleeva, M. P., Popov, I. Y. (2020a) Entanglement transmission through turbulent atmosphere for modes of Gaussian beam. *Quantum Information Processing*, 19 (2), article 72. <https://doi.org/10.1007/s11128-019-2569-y> (In English)
- Faleeva, M. P., Popov, I. Y. (2020b) On quantum bit coding by Gaussian beam modes for the quantum key distribution. *Nanosystems: Physics, Chemistry, Mathematics*, 11 (6), 651–658. <https://doi.org/10.17586/2220-8054-2020-11-6-651-658> (In English)
- Faleeva, M. P., Popov, I. Y. (2022) Singular numbers, entangled qubits transmission through a turbulent atmosphere and teleportation. *Indian Journal of Physics*, 96 (8), 2501–2505. <https://doi.org/10.1007/s12648-021-02143-9> (In English)
- Fedrizzi, A., Ursin, R., Herbst, T. et al. (2009) High-fidelity transmission of entanglement over a high-loss free-space channel. *Nature Physics*, 5, 389–392. <https://doi.org/10.1038/nphys1255> (In English)
- Gilev, P. A., Popov, I. Y. (2019) Quantum image transmission based on linear elements. *Nanosystems: Physics, Chemistry, Mathematics*, 10 (4), 410–414. <https://doi.org/10.17586/2220-8054-2019-10-4-410-414> (In English)
- Gumberidze, M. O., Semenov, A. A., Vasylyev, D., Vogel, W. (2016) Bell nonlocality in the turbulent atmosphere. *Physical Review A*, 94 (5), article 053801. <https://doi.org/10.1103/PhysRevA.94.053801> (In English)
- Heersink, J., Marquardt, Ch., Dong, R. et al. (2006) Distillation of squeezing from non-gaussian quantum states. *Physical Review Letters*, 96 (25), article 253601. <https://doi.org/10.1103/PhysRevLett.96.253601> (In English)
- Herbst, T., Scheidl, T., Fink, M. et al. (2015) Teleportation of entanglement over 143 km. *Proceedings of National Academy of Sciences*, 112 (46), 14202–14205. <https://doi.org/10.1073/pnas.1517007112> (In English)
- Ishimaru, A. (1978) *Wave propagation and scattering in random media. Vol. 1*. New York: Academic Press, 339 p. <https://doi.org/10.1016/B978-0-12-374701-3.X5001-7> (In English)
- Mandel, L., Wolf, E. (1995) *Optical coherence and quantum optics*. Cambridge: Cambridge University Press, 1192 p. (In English)
- Mattle, K., Weinfurter, H., Kwiat, P. G. et al. (1996) Dense coding in experimental quantum communication. *Physical Review Letters*, 76 (25), article 4656. <https://doi.org/10.1103/PhysRevLett.76.4656> (In English)
- Nielsen, M. A., Chuang, I. L. (2010) *Quantum computation and quantum information*. Cambridge: Cambridge University Press, 670 p. (In English)
- Peters, N., Altepeter, J., Jeffrey, E. et al. (2003) Precise creation, characterization, and manipulation of single optical qubits. *Quantum Information Computation*, 3, 503–518. <https://doi.org/10.48550/arXiv.quant-ph/0502177> (In English)
- Schleich, W. P. (2001) *Quantum optics in phase space*. Berlin: WILEY-VCH Verlag, 695 p. <https://doi.org/10.1002/3527602976> (In English)
- Semenov, A. A., Turchin, A. V., Gomonay, H. V. (2008) Detection of quantum light in the presence of noise. *Physical Review A*, 78 (5), article 055803. <https://doi.org/10.1103/PhysRevA.78.055803> (In English)
- Semenov, A. A., Turchin, A. V., Gomonay, H. V. (2009) Erratum: Detection of quantum light in the presence of noise [Phys. Rev. A 78, 055803 (2008)]. *Physical Review A*, 79 (1), article 019902. <https://doi.org/10.1103/PhysRevA.79.019902> (In English)
- Semenov, A. A., Vogel, W. (2009) Quantum light in the turbulent atmosphere. *Physical Review A*, 80 (2), article 021802(R). <https://doi.org/10.1103/PhysRevA.80.021802> (In English)
- Semenov, A. A., Vogel, W. (2010) Entanglement transfer through the turbulent atmosphere. *Physical Review A*, 81 (2), article 023835. <https://doi.org/10.1103/PhysRevA.81.023835> (In English)
- Soderholm, J., Bjork, G., Klimov, A. B., Sanchez-Soto, L. L., Leuchs, G. (2012) Quantum polarization characterization and tomography. *New Journal of Physics*, 14 (11), article 115014. <https://doi.org/10.1088/1367-2630/14/11/115014> (In English)
- Tatarskii, V. I. (1971) *Effect of the turbulent atmosphere on wave propagation*. Jerusalem: Israel Program for Scientific Translations Publ., 488 p. (In English)
- Ursin, R., Tiefenbacher, F., Schmitt-Manderbach, T. et al. (2007) Entanglement-based quantum communication over 144 km. *Nature Physics*, 3 (7), 481–486. <https://doi.org/10.1038/nphys629> (In English)
- Vasylyev, D., Semenov, A. A., Vogel, W. (2016) Atmospheric quantum channels with weak and strong turbulence. *Physical Review Letters*, 117 (9), article 090501. <https://doi.org/10.1103/PhysRevLett.117.090501> (In English)
- Williams, B., Sadlier, R., Humble, T. (2018) Superdense coding for quantum networking environments. *Proceedings. Vol. 10547. Advances in Photonics of Quantum Computing, Memory, and Communication XI*. San Francisco: SPIE OPTO Publ., article 105470B. <https://doi.org/10.1117/12.2295016> (In English)